AD-A046 790 NAVAL RESEARCH LAB WASHINGTON D C F/G 4/2
AN EFFICIENT NUMERICAL MODEL OF THE PLANETARY ATMOSPHERIC BOUND--ETC(U)
SEP 77 T YU, D STROBEL

UNCLASSIFIED NRL-MR-3603 NL

| OF |
AD
A046 790

END
DATE
FILMED
12-77
DDC

(12) R.S.

NRL Memorandum Report 3603

(6)

An Efficient Numerical Model of the Planetary Atmospheric Boundary Layer.

(10) TSANN-WANG YU

JAYCOR
205 S. Whiting Street
Alexandria, VA 22304

and

DARRELL STROBEL

Plasma Dynamics Branch
Plasma Physics Division

(14) NRL-MR-3603

(9) Interim rept.,

(12) 32 p.

(11) Sep[redacted]77

(16) F52552

(17) WF52552713

NAVAL RESEARCH LABORATORY
Washington, D.C.

251 950

SECURITY CLASSIFICATION OF THIS PAGE (When Data Entered)

REPORT DOCUMENTATION PAGE

READ INSTRUCTIONS BEFORE COMPLETING FORM

1. REPORT NUMBER: NRL Memorandum Report 3603
2. GOVT ACCESSION NO.:
3. RECIPIENT'S CATALOG NUMBER:

4. TITLE (and Subtitle): AN EFFICIENT NUMERICAL MODEL OF THE PLANETARY ATMOSPHERIC BOUNDARY LAYER

5. TYPE OF REPORT & PERIOD COVERED: Interim report on a continuing NRL problem.

6. PERFORMING ORG. REPORT NUMBER:

7. AUTHOR(s): Tsann-Wang Yu, JAYCOR, and Darrell Strobel, NRL

8. CONTRACT OR GRANT NUMBER(s):

9. PERFORMING ORGANIZATION NAME AND ADDRESS: Naval Research Laboratory, Washington, D.C. 20375

10. PROGRAM ELEMENT, PROJECT, TASK AREA & WORK UNIT NUMBERS: NRL Problem A03-23, Task WF 52-552-713

11. CONTROLLING OFFICE NAME AND ADDRESS: Naval Air Systems Command, Washington, D.C. 20361

12. REPORT DATE: September 1977

13. NUMBER OF PAGES: 31

14. MONITORING AGENCY NAME & ADDRESS (if different from Controlling Office):

15. SECURITY CLASS. (of this report): UNCLASSIFIED

15a. DECLASSIFICATION/DOWNGRADING SCHEDULE:

16. DISTRIBUTION STATEMENT (of this Report): Approved for public release; distribution unlimited.

17. DISTRIBUTION STATEMENT (of the abstract entered in Block 20, if different from Report):

18. SUPPLEMENTARY NOTES:

19. KEY WORDS (Continue on reverse side if necessary and identify by block number):
Boundary layer
Modeling
Turbulence
Parameterization

20. ABSTRACT (Continue on reverse side if necessary and identify by block number):
This paper presents an efficient two-dimensional time-dependent one-layer boundary layer model designed specifically for use in general circulation models. Two fundamental problems associated with the boundary layer parameterization are examined using the one-dimensional version of the model. These are the effects of different PBL parameterization schemes and different flux profiles on the model wind and temperatures. This paper concludes that the effect of different PBL parameterization is very significant on temperature calculation but less important on the wind speed.

over

(Continues)

DD FORM 1 JAN 73 1473 EDITION OF 1 NOV 65 IS OBSOLETE
S/N 0102-014-6601

SECURITY CLASSIFICATION OF THIS PAGE (When Data Entered)

20. Abstract (Continued)

In general, the use of linear flux profiles for the vertical divergence of momentum, heat and moisture is found to be satisfactory. We conclude this study by testing the validity of our two-dimensional model by comparing it with multi-level boundary layer model results. For this purpose, a numerical integration was done to simulate a stably stratified air flow passing from smooth to rough surfaces.

CONTENTS

AN EFFICIENT NUMERICAL MODEL OF THE PLANETARY ATMOSPHERIC BOUNDARY LAYER

1. INTRODUCTION

There are two general approaches to develop numerical models of the atmospheric boundary layer. The most common approach has been the construction of a multi-level boundary layer model (e.g. Estoque, 1963, Sasamori, 1971), when detailed structures of the planetary boundary layer (PBL) wind and temperature are required. For global circulation studies, however, the multi-level PBL models may not be practical in view of the computational demands. The alternative is to develop more efficient models with one or two levels in the vertical specifically designed for parameterizing the bulk properties of the PBL for use in large scale atmospheric circulations, (Randall, 1976; Benoit, 1976; Stull, 1977). This paper will describe an efficient two-dimensional, time-dependent, one-level boundary layer model suitable for global circulation studies.

Two fundamental problems associated with the PBL parameterization are determinations of the surface fluxes and the effect of flux profiles in the interior of the PBL. Several different schemes are being used for parameterizing the boundary layer fluxes (see e.g. Bhumralkar, 1976). The simplest ones employ the usual bulk transfer relations with all the transfer coefficients for drag C_D and heat C_H assumed equal and prescribed a priori. In some cases different values are assigned for land and ocean surfaces and also some allowance is made for different stability conditions. But by and large, these parameterization schemes are very crude.

Note: Manuscript submitted August 30, 1977.

Better schemes have been formulated from similarity considerations of the boundary layer. The basic assumptions underlying all similarity theories are that the boundary layer flow is horizontally homogeneous and quasi-stationary, a very restrictive assumption for many real atmospheric situations. As pointed out by Arya (1977), in a GCM, however, the variables are considered to be averaged horizontally over a fairly large grid area, and thus the assumption of horizontal homogeneity is probably well justified. Another alternative form of the similarity parametric relation originally proposed by Deardorff (1972) uses the layer-averaged wind, temperature and humidity. According to this approach, the drag and heat transfer coefficients C_D and C_H are calculated based on some nomograms. Numerical results based on this approach will be compared with those generated by the Rossby similarity theory.

Determination of the shapes of the turbulent flux profiles in the interior of the PBL is needed when the interface between the GCM grid layers lie within the PBL. The most common approach has been to prescribe the flux profiles as a linear function of height. This approach perhaps is adequate during the daytime convective hours when temperature stratifications are nearly adiabatic. However, during other stability conditions, the linear flux profile assumption may not be valid. Thus, another purpose of this paper is to investigate the effect of different vertical profiles of turbulent fluxes on model winds and temperatures.

Finally, we shall conclude this study by testing the validity of our model by comparing it with multi-level boundary layer model results. For this purpose, we shall simulate a stably stratified air flow passing from smooth to rough surfaces.

2. THE GOVERNING EQUATIONS

The model configuration is shown in Fig. 1. At the top of the boundary layer, i.e., $z = H$, the following boundary layer characteristics are assumed: (1) the wind speed is in geostrophic balance and the atmospheric pressure is constant in time and along the x-direction. (2) The temperature and humidity fields remain unchanged throughout the whole integration period.

At the level $z = H/2$, the boundary layer mean wind, temperature, and humidity are governed by the following equations:

$$\frac{\partial u}{\partial t} + u\frac{\partial u}{\partial x} + w\frac{\partial u}{\partial z} = -\frac{1}{\rho}\frac{\partial p}{\partial x} + fv - \frac{\partial}{\partial z}\overline{u'w'} \tag{1}$$

$$\frac{\partial v}{\partial t} + u\frac{\partial v}{\partial x} + w\frac{\partial v}{\partial z} = U_g - fu - \frac{\partial}{\partial z}\overline{v'w'} \tag{2}$$

$$\frac{\partial \theta}{\partial t} + u\frac{\partial \theta}{\partial x} + w\frac{\partial \theta}{\partial z} = -\frac{\partial}{\partial z}\overline{w'\theta'} \tag{3}$$

$$\frac{\partial q}{\partial t} + u\frac{\partial q}{\partial x} + w\frac{\partial q}{\partial z} = -\frac{\partial}{\partial z}\overline{w'q'} \tag{4}$$

$$\frac{\partial u}{\partial x} + \frac{\partial w}{\partial z} = 0 \tag{5}$$

$$\frac{\partial}{\partial z}\left(\frac{p}{p_0}\right)^k = -\frac{kg}{R\theta}, \text{ where } k = R/C_p. \tag{6}$$

All the symbols listed in Appendix I carry their usual physical meanings. In deriving this set of equations, we have assumed that the atmosphere is in hydrostatic equilibrium.

At the ground surface Z = 0, the wind speed is required to be zero. The surface temperature T_g is determined by the surface energy budget equation which gives rise to the following predictive equation (Bhurmalkar, 1975),

$$T_g^{n+1} = T_g^n + \left\{ \frac{S-R-H-LE-(\frac{\lambda c \omega}{2})^{\frac{1}{2}}(T_g - \bar{T})}{\frac{C_1}{\Delta t} + 4\sigma T_g^3 + C_H(1 + \frac{L}{C_p} GW \frac{dq_s}{dT}) + (\frac{\lambda c \omega}{2})^{\frac{1}{2}}} \right\}^n \qquad (7)$$

Here $C_1 = C + (\lambda c/2\omega)^{\frac{1}{2}}$ and C is the volumetric heat capacity, λ is the thermal conductivity, $\bar{T}$ the average daily surface temperature, ω is the frequency of oscillation, Δt the time step, σ is the Stefan-Boltzmann constant, C_H is the geostrophic heat transfer coefficient, C_p is the specific heat capacity at constant pressure, and L is the latent heat of evaporation.

3. THE CLOSURE PROBLEMS

A. PBL Parameterization Schemes

To close the system of equations described in Section 2, the flux terms in equations (1) - (4) have to be parameterized. The general form of the drag and other transfer relations obtained from similarity arguments is,

$$\left.\begin{aligned} kU_h/u_* &= -(\ell n \hat{Z}_o + A) \\ kV_h/u_* &= -B \text{ sign} \cdot f \\ k(\theta_h - \theta_o)/\theta_* &= -(\ell n \hat{Z}_o + C) \\ k(q_h - q_o)/q_* &= -(\ell n \hat{Z}_o + D) \end{aligned}\right\}$$

in which A, B, C and D are some similarity functions depending on atmospheric stability. Recently, Yamada (1976) reexamined the similarity functions based on the Wangara data (Clarke et al., 1971). Under both the stable and unstable conditions, his proposed similarity functions show substantial improvement over the previous work of Deardorff and Melgarejo (1975) and Arya (1975). For this study, we shall use (8) to compute the surface fluxes based on Yamada's (1976) similarity functions.

It should be pointed out that the height of the atmospheric boundary layer h may affect the similarity functions. In fact, this is the factor differentiating the Rossby number similarity theory from the generalized similarity theory. In the Rossby number similarity theory, the boundary layer height is uniquely determined by a height u_*/f. In the generalized similarity theory, h is considered as an variable depending on such factors as diurnal heating, large-scale subsidence, large-scale advection of heat and moisture etc.. Recently, Yu (1977) compared these two similarity theories and concluded that for mid-latitude boundary layer flow, the Rossby number similarity theory is just as valid as in the generalized similarity theory. In this paper, we adopt the Rossby number similarity theory. We shall compare our model results with those based on the Deardorff (1972) scheme according to which the drag and heat transfer coefficients C_D and C_H are calculated by some nomograms as shown in Fig. 2.

B. Effects of PBL Parameterization on Model Winds and Temperatures

In this section, we shall test the schemes described in

Section 3A with our simple model and study their effects on the model winds and temperatures. For this purpose, it is sufficient to use the one-dimensional version of the model, i.e., all the advective terms in equations (1) - (6) are set to zero. The model was integrated for 24 hours with the following initial and boundary conditions:

Boundary conditions: At $Z = H = 500$ m

$u = U_g = 10$ m/s, $v = v_g = 0$ m/s

$\theta = \theta_H = 308^o$ K, $q = q_H = 10$ g/kg;

At $z = 0$, $u = v = 0$ and the surface temperature is predicted by (7).

Initial conditions: At $Z = H/2 = 250$ m,

$u = 8$ m/s, $v = 2$m/s

$\theta = 305^o$ K, $q = 12$ g/kg;

At $Z = 0$, $\theta_o = 300^o$ K, $q_o = 14$ g/kg

Numerical methods and finite difference equations are described in the Appendix II. The Crank Nicolson method is used to integrate the model with a 30 minute time step.

Fig. 3 shows model temperatures calculated by the Rossby number similarity theory and Deardorff (1972) schemes for two selected heights, i.e. $Z = 0$ and $Z = 2$ m. We see that a difference as large as 4^o K may result when different PBL parameterization schemes are used. For the model wind speed, a maximum of 2.5 m/s difference is found at $Z = 2$ m between results calculated with the Rossby number similarity theory and the Deardorff (1972) schemes. This is shown in Fig. 4. The difference in wind speed becomes smaller, being less than 1 m/s at $Z = 250$ m. However, the effect on the model temperature at $Z = 250$ m is still significantly large, being on the order of 3.5^o K.

This is illustrated in Fig. 5.

Fig. 6 shows the wind speed hodograph at Z = 250 m for the Rossby number similarity theory and Deardorff (1972) scheme. The veering of the crossisobaric angles for both cases are similar, but the speed for the Rossby number similarity theory is relatively larger than that for the Deardorff schemes. This may be explained by the difference in calculated surface fluxes of momentum and heat as shown in Table 1. We can see from Table 1 that momentum fluxes calculated by the Deardorff (1972) scheme are much larger than those calculated by the similarity theory. As a result, the wind speed at Z = 250 m is much reduced with more momentum transmitted downward. Thus, the wind speeds at the two-meter levels are larger in Deardorff (1972) scheme than predicted by the similarity theory (see Fig. 4).

The kinematic heat flux calculated by both methods shown in Table 1 deserves mention. During the daytime hours, i.e. 1200 - 1500, the kinematic heat fluxes calculated by Deardorff (1972) scheme show negative values indicating upward transfer of heat flux from the ground. On the other hand, the heat fluxes calculated by the similarity theory are positive implying a downward transfer of heat flux to the ground. This difference may be attributable to that Deardorff (1972) scheme uses the boundary layer mean potential temperature to calculate the heat fluxes whereas the similarity theory uses single layer values of potential temperature. This difference in the method of heat flux calculation produces the temperature discrepancy illustrated in Figs. 3 and 5. For temperature prediction in GCM, an error of 1^{o} K may be acceptable. However, from the above results, we see a difference of

3 to 4° K in temperature prediction occurs when different PBL parameterization schemes are used. This points out the need for improved atmospheric boundary layer parameterization schemes in general circulation models. Unfortunately there is not sufficient data to select which scheme is best in this study.

4. EFFECT OF DIFFERENT VERTICAL PROFILES OF FLUXES ON MODEL WINDS AND TEMPERATURES

We shall assume the following profile relationships, i.e.,

$$\overline{\zeta' w'} = \overline{\zeta' w'}_o \exp \{- m(z/H)^2\} \qquad (9)$$

where $\zeta' = (u', v', \theta', q')$, the subscript o indicates the surface values, and the parameter m prescribes the shapes of exponential profiles as shown in Fig. 7. From (9), it follows that at Z = H/2,

$$\frac{\partial}{\partial z} \overline{\zeta' w'} = - (m/H) \exp (- m/4) \overline{u' w'}_0 .$$

For linear profiles,

$$\frac{\partial}{\partial z} \overline{\zeta' w'} = - \overline{u' w'}_o / H$$

Thus, the ratio of the vertical gradient of fluxes between exponential profiles and linear profiles is m exp (- m/4). From Table 2, it can be seen that changing the value of m leads to the modification of vertical flux gradient of the linear profile. For example, with m = 1, the fluxes calculated by (9) will be 78 percent of that calculated by linear profiles, and with m = 4, the fluxes calculated by (9) will be about 147 percent of that calculated by linear profiles. It should be noted that with m = 1.4 and m = 8.6 the fluxes calculated by (9)

is nearly equal to that of the linear profile. We integrated the one-dimensional version of the model for 24 hours with three different values of m i.e., m = 1, m = 4 and m = 8.6 for the exponential flux profile relationship (9). It should be noted that the governing equations for all the cases are the same except the flux divergence terms in equations (1) through (4) are different due to different values of m.

Fig. 8 shows potential temperatures at Z = 250 m calculated with three different values of m. We see the difference in potential temperature between the linear flux profile (m = 8.6) and exponential flux profiles with m = 1 and m = 4 is about 2^{o} K. The difference in wind speed is negligibly small, being less than 1 m/s with the three different values of m. This suggests that the shapes of turbulent flux profiles is not critical in a PBL parameterization scheme. In general, the use of linear flux profiles may be sufficient for general circulation studies.

5. CHANGES IN SURFACE ROUGHNESS

The purpose of this section is to determine if a simple model can reproduce some of the important features of more sophisticated multi-level boundary layer models. Yu and Wagner (1975) in a numerical study concluded that when stably-stratified air flow passes over a rougher surface, the increased turbulent fluxes of heat induced by the increased surface drag can cause the formation of a heat island. The model described in Section 2 employs similar governing equations and numerical schemes as those of Yu and Wagner (1975). The only difference between these two models is the number of levels in the vertical.

While our model has only one level, the model of Yu and Wagner (1975) had 21 levels. We shall thus simulate a stratified flow passing over a change in surface roughness as shown in Table 3. The boundary conditions are:

At $Z = H = 500$ m; $u(x,H) = U_g = 10$ m/s;

$v(x, H) = V_g = 0$; $\theta(x, H) = \theta_H = 308^o$ K;

$w(x, H) = 0$; and $p(x, H) = P_H = 900$ mb

At $z = 0$; $u(x, 0) = v(x, 0) = w(x, 0) = 0$;

$\theta(x, 0)$ = predicted by equation (7).

At the upwind lateral boundary, the variables u, v, θ are assumed to be uniform along the x-direction, and are obtained from the one-dimensional time-dependent version of the model. At the outflow lateral boundary, the upstream differencing scheme does not require boundary values. The initial conditions are:

At $Z = H/2 = 250$ m; $u(x, z) = 8$ m/s;

$v(x, z) = 2$ m/s; $\theta(x, z) = 305^o$ K

At $Z = 0$; $\theta(x, 0) = 300^o$ K

The finite difference equations are given in Appendix II. An implicit backward-time, upstream space finite difference scheme with a 30 minute time step is used to integrate the model.

Fig. 9 shows the calculated diurnal temperature variation at two locations, i.e. X = 1 and X = 5. Referring to Table 3, we see at X = 1, the roughness length is 0.001 m, while at X = 5, the roughness length is 2 m. From Fig. 9, it is evident that over the rougher surface, due to increased turbulent drag and heat flux transfer, the

air is well mixed near the surface during both day and night. Thus the difference in temperature between Z = 0 and Z = 2 m is very small at Z = 5. At the upstream boundary, i.e. Z = 1, temperature difference between Z = 0 and Z = 2 m is large especially during the nighttime. The most interesting feature is that during the stable hours, (18 - 06), the temperature at X = 5 is much warmer than that at X = 1. This is attributable to the fact that when a stably-stratified air passes over a rougher surface, the energy is redistributed due to increased turbulence mixing. This redistribution of heat results in the formation of a heat island. During the most unstable hours (12 - 16), we notice that the temperature near the surface up to 2 m over the rougher surface (X = 5) is cooler than that at X = 1. This is due to that intensive upward energy transfer occuring over the rougher surface results in less energy available for heating the air near the surface. These conclusions in general are in good agreement with the numerical results of Yu and Wagner (1975).

6. SUMMARY AND CONCLUSIONS

This paper presents an efficient two-dimensional time dependent one-layer boundary layer model especially designed for use in general circulation models. The one-dimensional version of the model was employed to examine the effect of different PBL parameterization schemes on the model winds and temperatures. Two PBL parameterization schemes considered to be more suitable for use in GCM studies were tested, namely, the Rossby number similarity theory and Deardorff (1972) schemes. The effect of using different PBL parameterization schemes is found to be very significant on temperature prediction but

not so much on the wind speed. Comparison of the numerical results using these two different PBL parameterization schemes shows a maximum difference of 4^{o} K in the temperature prediction. This difference is attributable to the large difference in the determination of surface momentum and heat fluxes. The fluxes of momentum and heat calculated by the similarity theory are much smaller than those of Deardorff (1972) scheme. In particular, during the unstable hours, the heat fluxes calculated by the Deardorff (1972) scheme are negative implying a upward transfer of heat energy. By the similarity theory, the heat fluxes are calculated to be positive during the unstable hours indicating a downward transfer of heat energy. This fundamental discrepancy has to be resolved by comparing results with observations. Clarke (1974) did a comparison between these two parameterization schemes using the Wangara experiment data and concluded that the similarity theory was more reliable.

The effect of different vertical profiles in turbulent fluxes on model wind and temperature was determined using the one-dimensional version of the model. It was concluded that the effect was less important and for general circulation studies, a linear profile might be adequately sufficient.

The two-dimensional model was used to simulate a stably-stratified air flow passing over from a smooth to a rougher surface. This was done to see if our model was capable of producing the same physical results as those by more sophisticated multi-level boundary layer models. It was concluded that our numerical results agree essentially with those of Yu and Wagner (1975) in that when stably stratified

flow passing over a rougher surface, the increased surface drag and thus the increased turbulent mixing can cause a heat island formation.

ACKNOWLEDGEMENTS

The authors would like to express their thanks to Drs. Mark Schoeberl of Science Application, Inc. and Rao Madala of the Naval Research Laboratory for their helpful discussions during the course of this research. This work was supported by the Naval Air System Command Task No. WF 52-552-713.

REFERENCES

Arya, S. P. S., 1975: Geostrophic drag and heat transfer relations for the atmospheric boundary layer. Quart. J. Roy. Meteor. Soc., 101, 147-161.

Arya, S. P. S., 1977: Suggested revision to certain boundary layer parameterization schemes used in atmospheric circulation models. Mon. Wea. Review, 105, 215-227.

Benoit, R., 1976: A comprehensive parameterization of the atmospheric boundary layer for general circulation models. NCAR Cooperative Thesis No. 39, 278 pp.

Bhurmalkar, C. M., 1975: Numerical experiments on the computation of ground surface temperature in an atmospheric general circulation model. J. Appl. Meteor. 14, 1246-1258.

Bhurmlakar, C. M., 1976: Parameterization of the planetary boundary layer in atmospheric general circulation models. Review Geophy. Space Phys., 14, 215-226.

Clark. R. H., 1974: Attempts to simulate the diurnal course of meteorological variables in the boundary layer. Irv. Atmos. and Oceanic Phys., 10, 600-612.

Clark, R. H., A. J. Dyer, R. R. Brook, D. G. Ried, and A. J. Troup, 1971: The Wangara experiment: Boundary layer data. Tech. Paper No. 19, CSIRO, Div. Meteor. Phys., Melbourne, Australia, 362 pp.

Deardorff, J. W., 1972: Parameterization of the planetary boundary layer for use in general circulation models. Mon. Wea. Rev., 100, 93-106.

Estoque, M., 1963: A numerical model of the atmospheric boundary layer. J. Geophy. Res., 68, 1103-1113.

Melgarejo, J. W., and J. W. Deardorff, 1974: Stability functions for the boundary-layer resistance laws based upon observed boundary layer heights. J. Atmos. Sci., 31, 1324-1333.

Sasamori, T., 1971: A numerical study of atmospheric and soil boundary layers. J. Atmos. Sci., 27, 1122-1137.

Stull, R. B., 1977: A planetary boundary layer parameterization for use in global forecast models, paper presented in the Third Conference on Numerical Weather Prediction of the American Meteorological Society, hold at Omaha, Nebraska, April 26-28, 1977.

Yamada, T., 1976: On the similarity functions A, B, and C of the planetary boundary layer. J. Atmos. Sci., 33, 781-793.

Yu, T. W., 1972: Two-dimensional time-dependent numerical simulation of atmospheric flow over an urban area. Ph.D. Dissertation, The University of Texas at Austin, 114 pp.

Yu, T. W., 1977: Determination of boundary layer fluxes based on similarity theories. Submitted to Mon. Wea. Rev. for publication.

Yu, T. W., and [illegible] 1975: Numerical study of the nocturnal boundary [illegible] Layer Meteor. 9, 143-162.

APPENDIX I

List of Symbols

C_D	geostrophic drag coefficient
C_H	geostrophic heat transfer coefficient
C_p	specific heat capacity at constant pressure
f	Coriolis parameter
g	gravitational acceleration
h	height of the model upper boundary
H	height of the model upper boundary, or sensible heat flux
I	space index for the x-direction
k	space index for the z-direction
n	time index for the finite difference equations
p	atmospheric pressure
P_o	atmospheric pressure of 1000 mb
q	specific humidity of air
q_o	specific humidity of air at surface
q_s	saturated specific humidity of air
q_*	surface friction humidity
t	time
T_q	surface temperature
u,v,w	velocity components in the x-, y-, and z-directions, respectively
U_h, V_h	velocity components in the x-, y-directions respectively at Z = h
u_*	surface friction velocity

x, y, z	coordinates in the downwind, cross-wind, and vertical directions respectively
Z_o	surface roughness parameter
$\hat{Z}_o$	normalized surface roughness parameter ($= Z_o/h$)
θ	potential temperature
θ_h	potential temperature at $Z = h$
θ_*	friction potential temperature
ρ	air density
$\hat{}$	latest available values in the iteration schemes
$-$	mean values
$/$	deviations from the mean values

APPENDIX II

Finite Difference Equations

1. The Model Equations

$$\frac{\partial u}{\partial t} + u\frac{\partial u}{\partial x} + w\frac{\partial u}{\partial z} = -\frac{1}{\rho}\frac{\partial p}{\partial x} + fv - \frac{\partial}{\partial z}\overline{u'w'}$$

$$\frac{\partial v}{\partial t} + u\frac{\partial v}{\partial x} + w\frac{\partial v}{\partial z} = -fu_g - \frac{\partial}{\partial z}\overline{v'w'}$$

$$\frac{\partial \theta}{\partial t} + u\frac{\partial \theta}{\partial x} + w\frac{\partial \theta}{\partial z} = -\frac{\partial}{\partial z}\overline{w'\theta'}$$

$$\frac{\partial q}{\partial t} + u\frac{\partial q}{\partial x} + w\frac{\partial q}{\partial z} = -\frac{\partial}{\partial z}\overline{w'q'}$$

$$\frac{\partial u}{\partial x} + \frac{\partial w}{\partial z} = 0$$

$$\frac{\partial}{\partial z}\left(\frac{P}{P_o}\right)^k = -\frac{kq}{R\theta}, \text{ where } k = R/C_p$$

2. Finite Difference Equations

A. At the lateral inflow boundary, i.e. X(1), the advective terms and vertical motion are zero. The finite difference equations may be written for the Crank-Nicolson schemes.

$$\frac{u^{n+1} - u^n}{\Delta t} = \frac{1}{2}\left(fv^{n+1} - fv_g^{n+1} + fv^n - fv_g^n\right) - \left(\frac{\partial}{\partial z}\overline{u'w'}\right)^{n+1}$$

$$\frac{v^{n+1} - v^n}{\Delta t} = \frac{1}{2}\left(fu_g^{n+1} - fu^{n+1} + fu_g^n - fu^n\right) - \left(\frac{\partial}{\partial z}\overline{v'w'}\right)^{n+1}$$

$$\frac{\theta^{n+1} - \theta^n}{\Delta t} = \left(-\frac{\partial}{\partial z}\overline{w'\theta'}\right)^{n+1}$$

$$\frac{q^{n+1} - q^n}{\Delta t} = \left(- \frac{\partial}{\partial z} \overline{w'q'} \right)^{n+1}$$

B. At the interior grid points, i.e. X(2) to X(N), the upstream finite difference scheme will be used, i.e.,

$$u \frac{\partial u}{\partial x} \simeq u(I,k) \frac{u(I,k) - u(I-1, k)}{x(I) - x(I-1)}, \text{ if } u > 0$$

$$u \frac{\partial u}{\partial x} \simeq u(I, k) \frac{u(I+1, k) - u(I,k)}{x(I+1) - x(I)}, \text{ if } u < 0$$

Note that using the upstream finite difference scheme requires no outflow boundary conditions.

The finite difference equations for $u > 0$ may be written as,

$$\frac{u^{n+1}(I, k) - u^n(I, k)}{\Delta t} = - \hat{u}^{n+1}(I, k) \frac{u^{n+1}(I, k) - u^{n+1}(I-1, k)}{x(I) - x(I-1)}$$

$$- \hat{w}^{n+1}(I, k) \frac{u^{n+1}(I, k+1) - u^{n+1}(I, k-1)}{z(k+1) - z(k-1)} + f v^{n+1}(I, k)$$

$$- \left(\frac{\partial}{\partial z} u'w' \right)^{n+1} - \frac{1}{\rho} \frac{P^{n+1}(I, k) - P^{n+1}(I-1, k)}{x(I) - x(I-1)}$$

$$\frac{v^{n+1}(I, k) - v^n(I, k)}{\Delta t} = \hat{u}^{n+1}(I, k) \frac{v^{n+1}(I, k) - v^{n+1}(I-1, k)}{x(I) - x(I-1)}$$

$$- \hat{w}^{n+1}(I, k) \frac{v^{n+1}(I, k+1) - v^{n+1}(I, k-1)}{z(k+1) - z(k-1)} - f u^{n+1}(I, k)$$

$$- f U_g - \left(\frac{\partial}{\partial z} \overline{w'v'} \right)^{n+1}$$

$$\frac{\theta^{n+1}(I, k) - \theta^{n}(I, k)}{\Delta t} = - u^{n+1}(I, k)\frac{\theta^{n+1}(I, k) - \theta^{n+1}(I-1, k)}{x(I) - x(I-1)}$$

$$- \hat{w}^{n+1}(I, k)\ \frac{\theta^{n+1}(I, k+1) - \theta^{n+1}(I, k+1)}{z(k+1) - z(k-1)} - \left(\frac{\partial}{\partial z}\overline{w'\theta'}\right)^{n+1}$$

$$\frac{q^{n+1}(I, k) - q^{n}(I, k)}{\Delta t} = - \hat{u}^{n+1}(I, k)\ \frac{q^{n+1}(I, k) - q^{n+1}(I-1, k)}{x(I) - x(I-1)}$$

$$- \hat{w}^{n+1}(I, k)\frac{q^{n+1}(I, k+1) - q^{n+1}(I, k-1)}{z(k+1) - z(k-1)} - \left(\frac{\partial}{\partial z}\overline{w'q'}\right)^{n+1}$$

$$\text{at } z = H/2,\ P(I, k) = \left[P^{k}(I, k+1) + \frac{kgP_o^{\ k}}{2R}\left\{\frac{1}{\theta(I, k)} + \frac{1}{\theta(I, k+1)}\right\}\right]^{1/k}$$

$$\text{at } z = 0,\ P(I, k-1) = \left[P^{k}(I, k) + \frac{kgP_o^{\ k}}{2R}\left\{\frac{1}{\theta(I, k)} + \frac{1}{\theta(I, k-1)}\right\}\right]^{1/k}$$

3. Stability of the Finite Difference Equations

The finite difference equations described previously have been proved to be numerically stable with large time steps (see e.g. Yu (1972)).

Table 1: Momentum and kinematic heat fluxes calculated by the similarity theory and Dearodrff (1972) scheme

	MOMENTUM FLUX (u_*^2) (10^{-3} m^2 sec^{-2})		KINEMATIC HEAT FLUX ($u_*\theta_*$) (10^{-3} m sec^{-1} ^0K)	
Local Time	Similarity Theory	Deardorff (1972)	Similarity Theory	Deardorff (1972)
18	6.7	17.8	7.2	17.0
21	2.3	23.8	4.9	32.5
24	1.6	34.9	4.2	47.3
3	1.4	25.3	3.9	36.0
6	1.3	5.5	3.9	9.7
9	3.0	1.5	5.4	15.5
12	29.7	62.9	17.1	-9.9
15	29.3	70.8	17.1	-6.5
18	4.6	54.9	6.5	30.4

Table 2: The ratio between exponential flux profile and linear flux profile for different values of m

m	mexp(-m/4)	m	mexp(-m/4)
0	0	5	1.43
1	0.78	6	1.33
1.4	0.99	7	1.22
1.5	1.03	8	1.08
2	1.21	8.6	1.001
3	1.42	9	0.95
4	1.47	10	0.88

Table 3: Assumed variation in x-direction for roughness length

I	x(km)	Z_o(m)
1	0	0.001
2	5	0.001
3	10	1.00
4	15	1.00
5	20	2.00
6	25	1.00
7	30	1.00
8	35	0.001
9	40	0.001
10	45	0.001

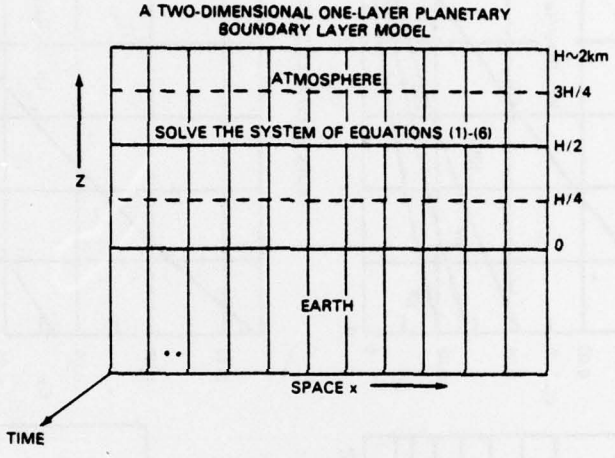

Fig. 1 – The model configuration

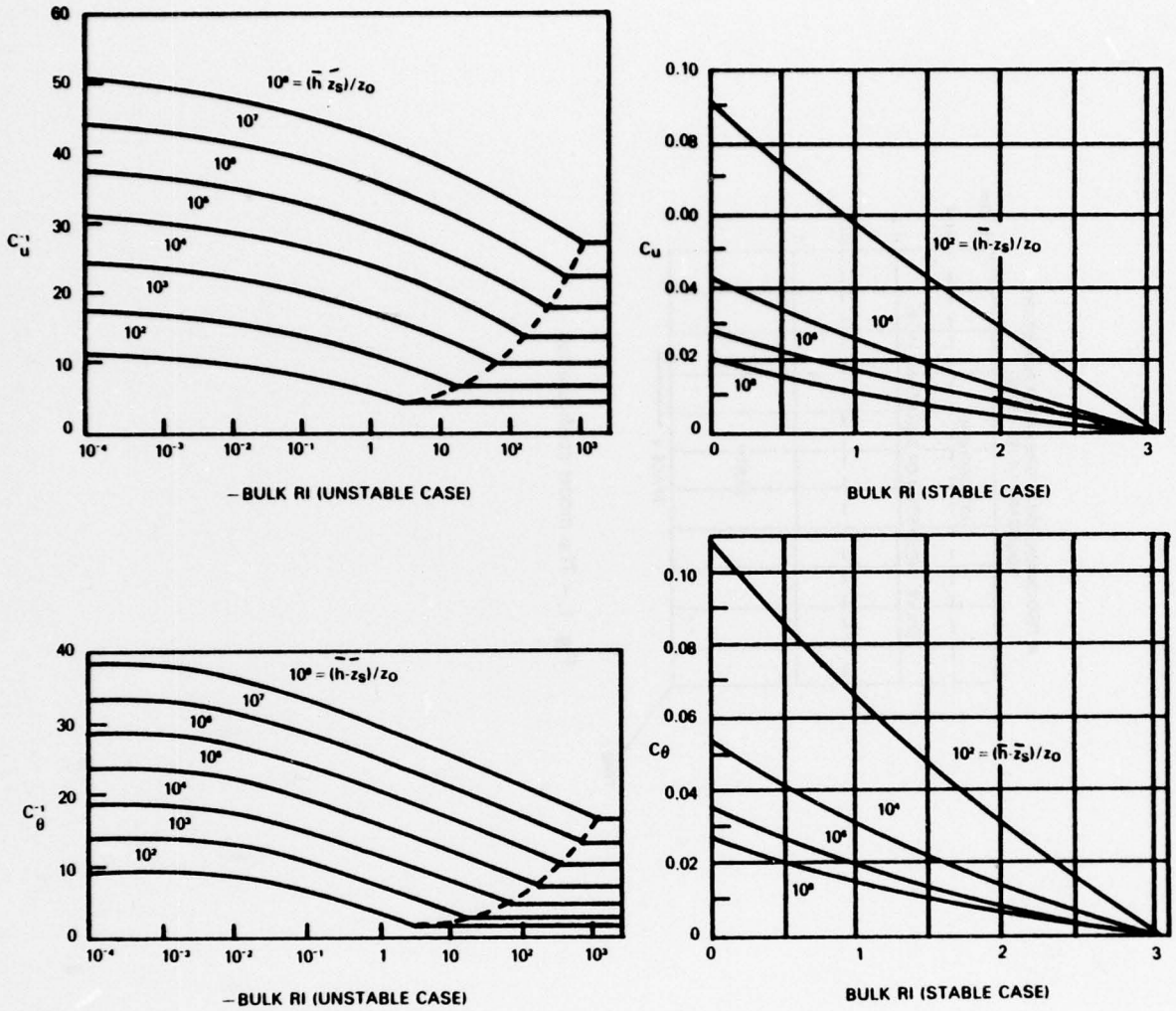

Fig. 2 – Nomograms for determining C_D and C_H based on Deardorff (1972) scheme

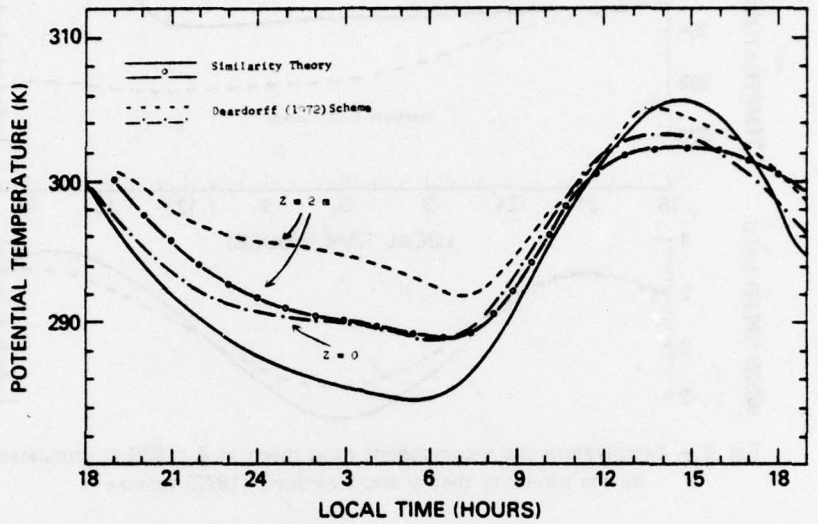

Fig. 3 – Potential temperature at two selected heights, i.e., Z = 0 and Z = 2 m calculated by the similarity theory and Deardorff (1972) scheme

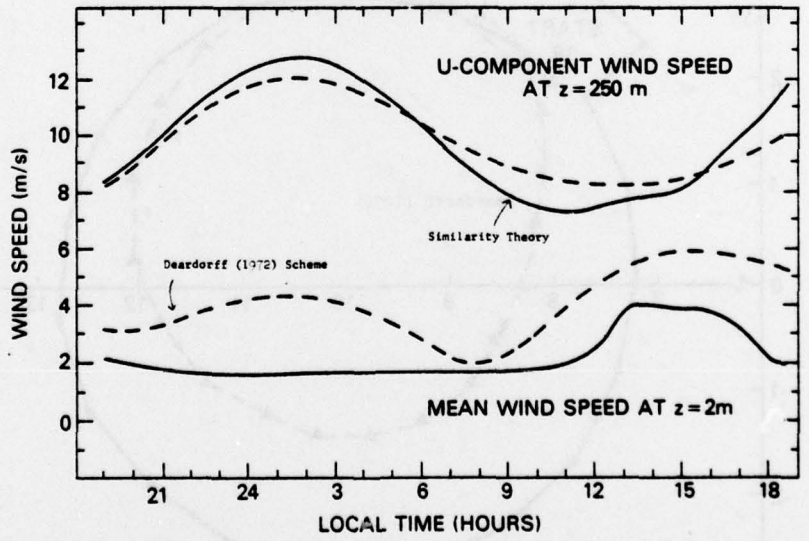

Fig. 4 – Two-meter mean wind speed and u-component wind speed at Z = 250 m calculated by the similarity theory and Deardorff (1972) scheme

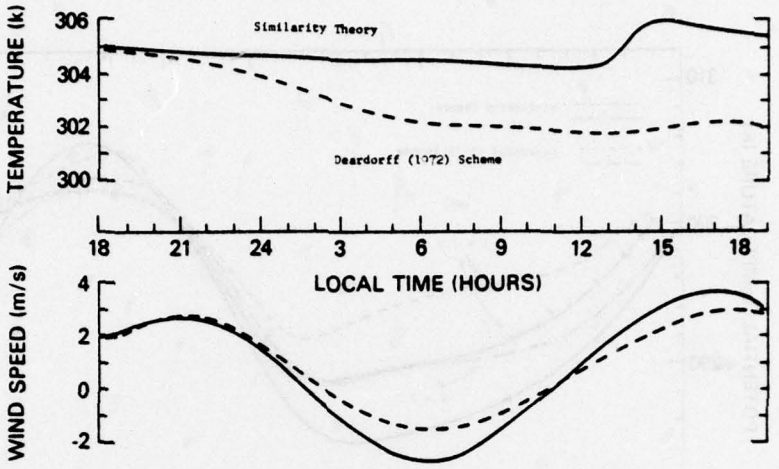

Fig. 5 – Temperature and v-component wind speed at Z = 250 m calculated by the similarity theory and Deardorff (1972) scheme

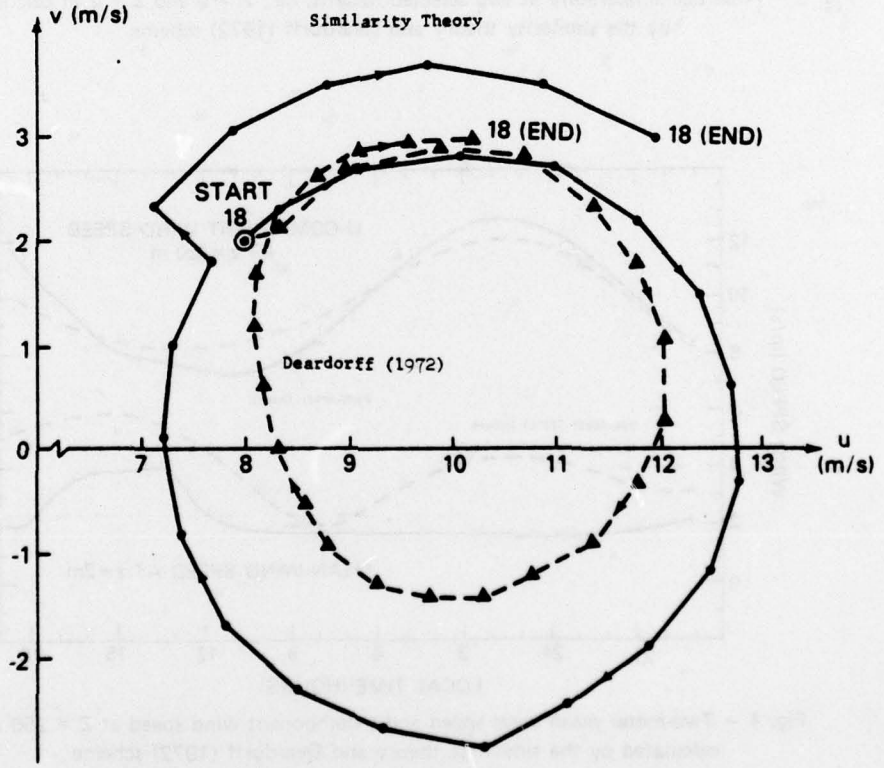

Fig. 6 – Wind hodographs at Z = 250 m calculated by the similarity theory and Deardorff (1972) scheme

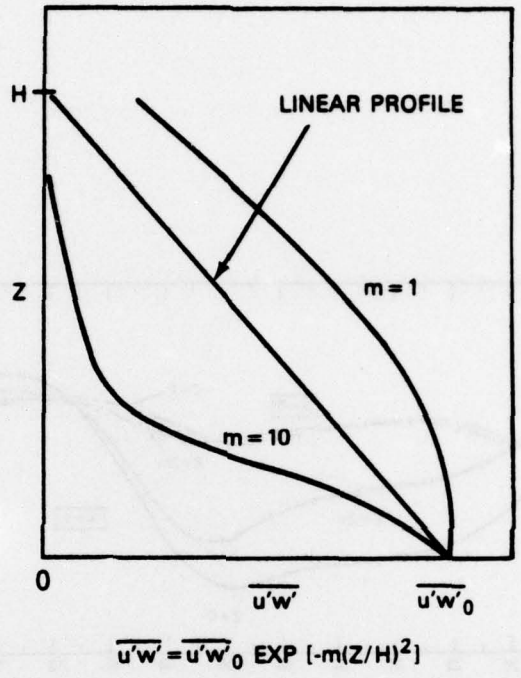

Fig. 7 – Different shapes of turbulent flux profile equation $\overline{u'w'} = \overline{u'w'_0}$ exp $[-m(z/H)^2]$

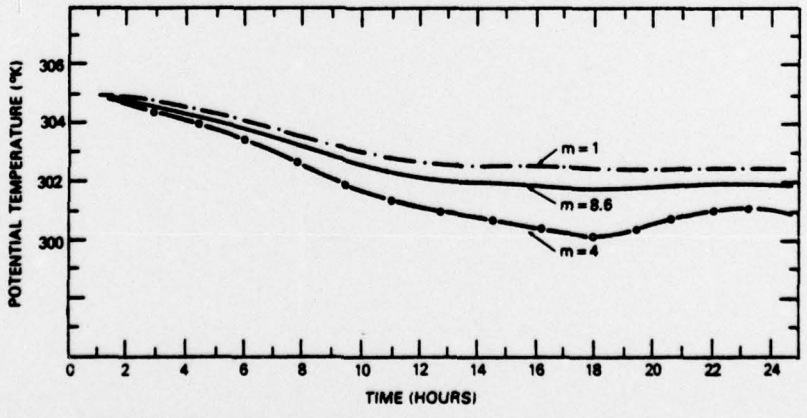

Fig. 8 – Effect of different shapes of turbulent flux profiles on potential temperature at Z = 250 m

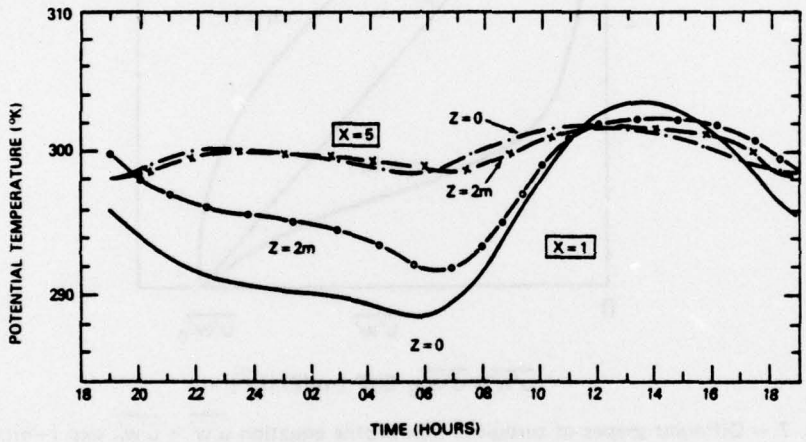

Fig. 9 — Diurnal variation of the surface and two-meter potential temperature at two selected locations x = 1 and x = 5